Receptor and βγ Binding Sites in the α Subunit of the Retinal G Protein Transducin

René Onrust,* Paul Herzmark, Patty Chi, Pablo D. Garcia, Olivier Lichtarge, Chris Kingsley, Henry R. Bourne†

Transmembrane receptors for hormones, neurotransmitters, light, and odorants mediate their cellular effects by activating heterotrimeric guanine nucleotide–binding proteins (G proteins). Crystal structures have revealed contact surfaces between G protein subunits, but not the surfaces or molecular mechanism through which Gαβγ responds to activation by transmembrane receptors. Such a surface was identified from the results of testing 100 mutant α subunits of the retinal G protein transducin for their ability to interact with rhodopsin. Sites at which alanine substitutions impaired this interaction mapped to two distinct Gα surfaces: a βγ-binding surface and a putative receptor-interacting surface. On the basis of these results a mechanism for receptor-catalyzed exchange of guanosine diphosphate for guanosine triphosphate is proposed.

Heterotrimeric G proteins relay signals from seven-transmembrane-spanning receptors (7TMRs) to cellular enzymes and ion channels. Activated by photons, odors, and many hormones and neurotransmitters, 7TMRs catalyze replacement by guanosine triphosphate (GTP) of guanosine diphosphate (GDP) bound to Gα subunits, causing dissociation of the Gα·GTP and βγ subunits, which in turn relay the signal to downstream effectors (*1*). Activation is robust; in the case of transducin (G_t), rhodopsin induces an ~10^7-fold increase in the basal (unstimulated) rate of GTP-GDP exchange (*2*). Crystal structures (*3*–*5*) have defined conserved folds of G proteins, as well as the trimeric structure, GTP-induced conformational change, and a plausible catalytic mechanism for GTP hydrolysis, which turns off the signal. It is not known, however, how the G protein interacts with its 7TMR and responds by exchanging GDP for GTP.

Biochemical and molecular genetic approaches have defined three key features of this interaction: (i) The 7TMR interacts directly with both βγ and Gα (*6*, *7*). (ii) The COOH-terminal tail of Gα (~10 residues) interacts directly with the receptor (*7*–*10*). (iii) In addition to the COOH-terminal tail, the interaction involves other residues in Gα not yet identified (*7*, *9*). Here we report results of a comprehensive molecular genetic strategy that confirm these findings and identify a putative 7TMR-interacting surface of Gα, and we suggest a mechanism for 7TMR-triggered conformational change.

We used two assays of G protein activation to test 100 Gα mutants in which alanine replaced individual amino acid residues in the α subunit of G_t (α_t) [92 single and 8 double replacements (*11*)]. In the crystal structure, almost all of these residues are oriented toward the solvent (*12*). The first assay measured the ability of rhodopsin, in the presence of all-*trans*-retinal, to promote guanosine 5′-O-(3′-triotriphosphate) (GTP-γ-S) binding to α_t in microsomal extracts from COS-7 cells transiently expressing α_t, β_1, γ_1, and opsin. Binding of GTP-γ-S induces a conformational change that is detected by the accumulation of a trypsin-resistant α_t fragment (Fig. 1) (*10*). The second assay (Fig. 2) assessed the ability of α_t, translated in vitro and labeled with [^{35}S]methionine, to bind photoactivated rhodopsin in membranes prepared from retinal rod outer segments (*13*). Activation by AlF_4^- served as a functional control in both assays.

The microsomal assay revealed unequiv-

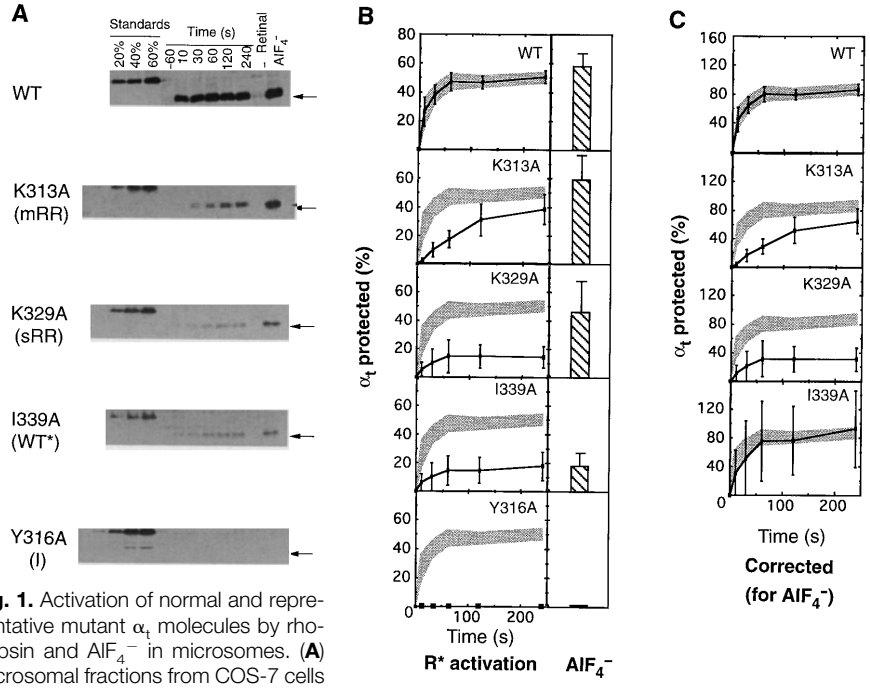

Fig. 1. Activation of normal and representative mutant α_t molecules by rhodopsin and AlF_4^- in microsomes. (**A**) Microsomal fractions from COS-7 cells expressing α_t alanine mutants, bovine opsin, β_1, and γ1 were incubated with all-*trans*-retinal under ambient light. Samples were removed at the indicated times before and after the addition of GTP-γ-S (10 μM) and treated with trypsin, as described (*10*). Lanes labeled "−Retinal" show the slow rate of GTP-γ-S–for–GDP exchange in the absence of photoactivated rhodopsin. Lanes labeled "AlF_4^-" represent incubations that contained AlF_4^-, but not GTP-γ-S (*10*). Arrows indicate the 31-kD trypsin-resistant α_t fragments. Standard lanes represent percentages of the original microsomal extract, not treated with trypsin. Abbreviations: WT, normal α_t; mRR, moderately impaired receptor response; sRR, severely impaired receptor response; WT*, normal interaction when assay results are corrected for a moderate decrease in protection by AlF_4^-; I, indeterminable activation by rhodopsin. For the mutant designations, A is Ala, I is Ile, K is Lys, and Y is Tyr, and the number indicates the position of the mutated residue. (**B**) Quantitative analysis (by densitometry of immunoblots) of α_t protection by activated rhodopsin (R*) or AlF_4^-. For each mutant, values represent the mean ± 2 SEM of at least four separate experiments, performed on microsomal membranes derived from at least two separate transfections. The shaded area depicts the range (mean ± 2 SEM) of results with normal α_t (WT) in the presence of all-*trans*-retinal. (**C**) Values of activation time courses, corrected for the amount of protection by AlF_4^- [calculated as the quotient of the uncorrected values divided by the mean values for AlF_4^- protection (*11*)].

Department of Cellular and Molecular Pharmacology, Department of Medicine, Programs in Cell Biology and Biomedical Sciences, and the Cardiovascular Research Institute, University of California, San Francisco, CA 94143–0450, USA.

*Present address: Genesis Research and Development, Post Office Box 50, Auckland, New Zealand.

†To whom correspondence should be addressed at S-1212, Box 0450, University of California Medical Center, San Francisco, CA 94143–0450, USA.

ocally impaired responses to rhodopsin in 24 of the 88 mutants (*11*) in which the effect of rhodopsin could be determined. We subclassified these (*11*) as severely or moderately impaired in receptor response (sRR or mRR); Fig. 1 depicts a representative sRR and an mRR phenotype. The remaining 64 mutants showed normal (WT) responses. Of the 54 in vitro–translated α_t mutants in which we could assess binding to photoactivated rhodopsin, 22 had impaired receptor binding (RB), whereas 32 phenotypes were WT. Autoradiograms and quantitation (by PhosphorImager) of α_t bound to rhodopsin, in the absence or presence of GTP-γ-S, for four representative mutants is shown in Fig. 2. In the presence of GTP-γ-S, considerably smaller amounts of [^{35}S]methionine-labeled normal (unmutated) α_t bound to rhodopsin, presumably because rhodopsin efficiently induces α_t to bind GTP-γ-S, putting it into a stable conformation that binds poorly to both βγ and to rhodopsin. For all mutants, classification into WT or RB categories was the same whether we assessed total α_t binding or the difference between binding in the absence or presence of GTP-γ-S (*14*).

As a control in both assays, α_t mutants were tested for susceptibility to protection from tryptic cleavage by a receptor-independent stimulus, AlF_4^- [which mimics the γ-phosphate of GTP, thereby switching GDP-bound Gα into a conformation that resists trypsin cleavage (*3, 4, 10, 15*)]. For some mutants in both assays, AlF_4^- protection was reduced but reproducible. In these cases we assessed the rhodopsin interaction phenotype by normalizing it relative to the degree of protection effected by AlF_4^- (Figs. 1 and 2, mutants I339A and D311A, respectively). With the normalization procedure we classified 15 and 7 mutant phenotypes as WT in the activation and binding assays, respectively. By the criterion of resistance to trypsin, small numbers of mutants failed to respond to AlF_4^- under each assay condition (12 of 100 and 12 of 66 in the microsomal and in vitro translation assays, respectively) (*16*). Rhodopsin activation or binding could not be assessed for these mutants, which are designated (*11*) indeterminable (I) (Y316A in Fig. 1, L349A in Fig. 2). The phenotypes of all but seven mutants could be determined in at least one of the assays (*16*). The informative 93 mutants were thus designated either R or WT, to indicate whether or not the mutation impaired interaction with rhodopsin (*11*).

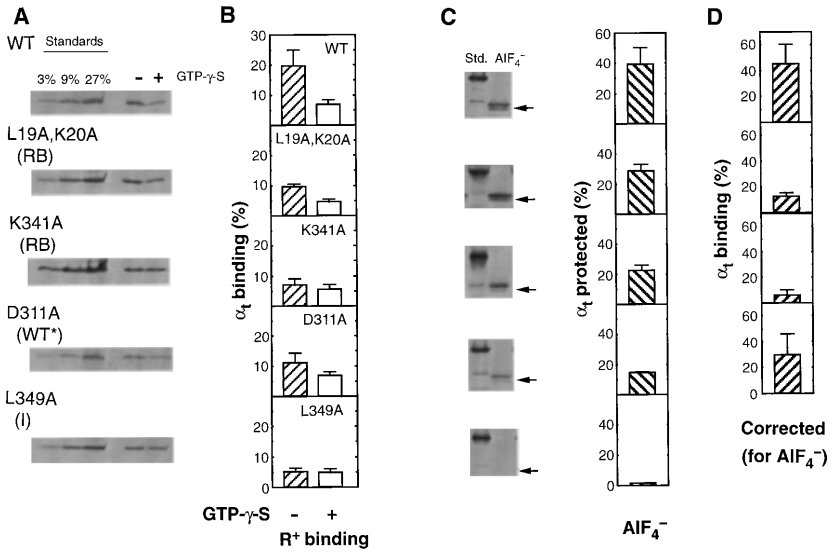

Fig. 2. Binding to photoactivated rhodopsin of normal and mutant α_t translated in vitro. (**A**) Samples of the diluted translation mix, containing [^{35}S]methionine-labeled α_t, were incubated with rod outer segment membranes in ambient light, in the presence or absence of GTP-γ-S, as described (*13*). Standard lanes represent percentages of total labeled α_t in the translation extract. Samples were subjected to SDS–polyacrylamide gel electrophoresis (SDS-PAGE) and autoradiography (*13*). For the mutant designations, D is Asp and L is Leu. (**B**) Quantitative analysis (by PhosphorImager) of binding results. R* binding depicts the percentage of total radiolabeled α_t bound to rhodopsin in the absence (−) or presence (+) of 100 μM GTP-γ-S. For each mutant, values represent the mean ± 2 SEM of at least four separate experiments, performed on in vitro–translated α_t derived from at least two separate preparations. (**C**) Autoradiograms and quantitative analysis of the percent of α_t protected from trypsin by AlF_4^-; arrows indicate the 31-kD trypsin-resistant α_t fragments. Std., standard (100% equivalent). (**D**) Corrected values of binding experiments for representative alanine mutants. Bars represent the difference between binding in the absence and the presence of GTP-γ-S, normalized with respect to protection by AlF_4^- (*11*).

To construct a three-dimensional (3D) model of G protein activation by 7TMRs (Fig. 3), we assigned to 34 R residues a specific role as components of binding surfaces that may interact directly with βγ or rhodopsin. Although any alanine substitution could indirectly hinder the interaction by blocking rhodopsin-induced conformational change, rather than by preventing binding of α_t to rhodopsin, assignments of several residues into the R category are in keeping with previous evidence (*5, 7, 9, 17*).

Mapped onto the crystal structure (*5*) of α_t, these 34 R residues form two sets of clusters. Our model assigns these to putative surfaces for interaction with βγ or with the 7TMR (Fig. 3, A through D). Both surfaces of α_t are probably similar in location and function to corresponding surfaces of other Gα molecules (*1, 4, 5, 7*). Indeed, the two surfaces functionally defined in our experiments closely match surfaces predicted (*18*) by inference from mapping residues conserved among Gα subunits onto the α_t 3D structure.

Rhodopsin and other 7TMRs appear to "act at a distance" (*18*) in catalyzing GTP-for-GDP exchange, in that intracellular loops of most 7TMRs are too short to allow direct interaction with the guanine nucleotide–binding site, which is probably located ~30 Å from the plasma membrane (Fig. 3, A and C). On the basis of the proposed βγ- and 7TMR-interacting surfaces, we devised an explanation for propagation of the conformational signal from the receptor to the nucleotide-binding pocket.

Most of the α_t residues that directly contact βγ in crystals of the heterotrimer (*5*) showed an R phenotype (*17*), confirming that the 17 R residues (cyan-colored in Fig. 3, A through C) coincide with the βγ-binding surface of α_t. βγ-interacting residues are distributed among four elements of secondary structure (*11*), three of which (Fig. 3, D and E) stretch from the postulated plane of the plasma membrane (*5, 18*) to the GDP-binding pocket. It is likely that βγ cooperates with the 7TMR to open the nucleotide-binding site, either actively, by inducing conformational change in Gα, or indirectly, by enhancing affinity of the Gαβγ complex for the 7TMR; in the latter role, βγ could also serve as a stabilizer or fulcrum to make Gα more susceptible to a separate action of the 7TMR.

A putative 7TMR-interacting surface (outlined in dark blue in Fig. 3) is located near the membrane, at the ends of α5 and β6 (that is, the COOH-terminal tail and the α4-β6 loop, respectively; Fig. 3, A through C). Additional mutation-sensitive sites located in both β6 and α5 extend part way toward the guanine nucleotide–bind-

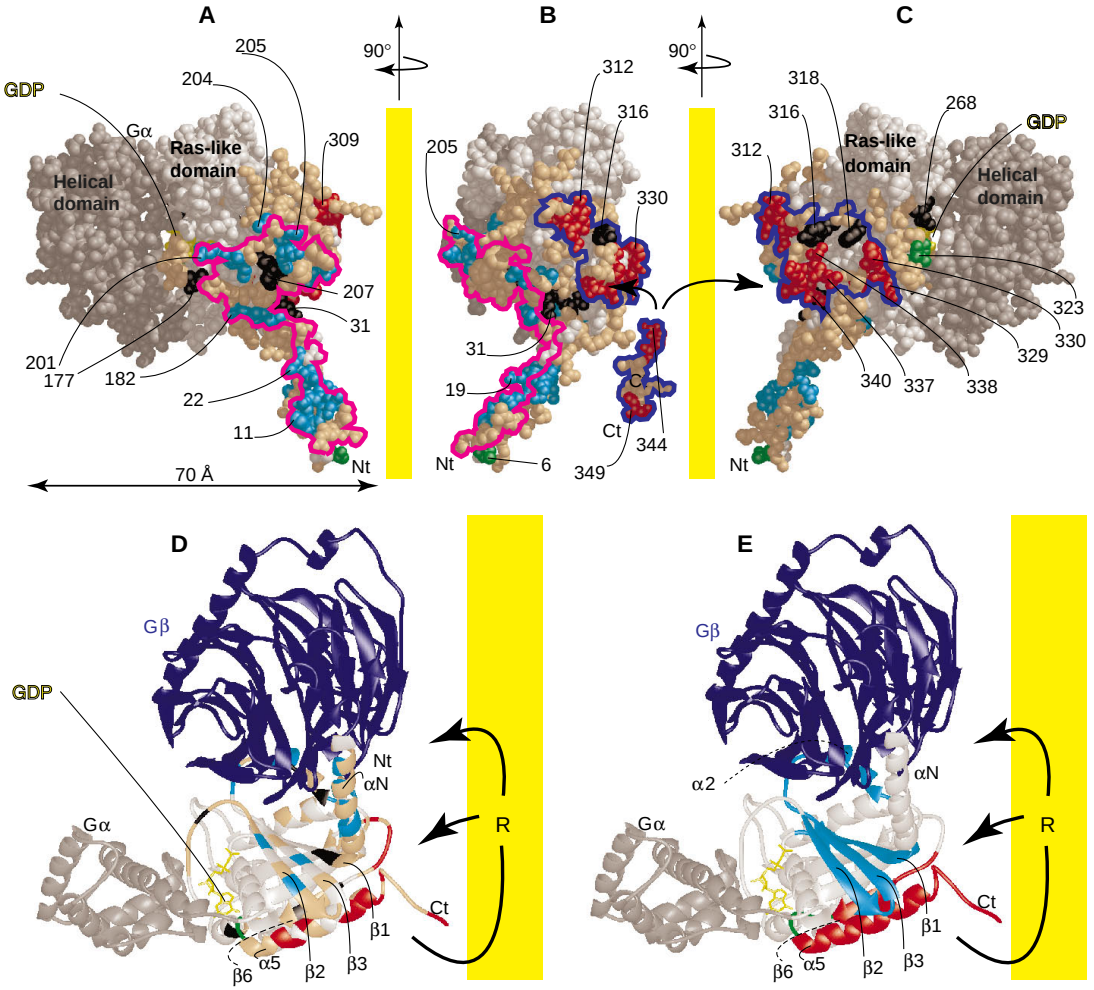

Fig. 3. Alanine mutations and 3D structure of α_t. (**A** to **C**) Views of α_t rotated successively by 90° about the vertical axis, which is parallel to the postulated (*5*, *18*) plane of the plasma membrane; the membrane presumably is located just to the right of the model in (A) and just to the left of the model in (C) (vertical yellow stripes). Panel (A) represents the face of α_t that binds to βγ and (B) the face of α_t that would be "seen" by the receptor in the membrane, whereas (C) depicts the face of α_t opposite to that seen in (A). Residues at sites where alanine substitution impaired interaction with rhodopsin are colored cyan (βγ-interacting surface, outlined in magenta), red (putative rhodopsin-interacting surface, outlined in dark blue), and green [other residues, as indicated in (*24*)]. Beige or black indicate, respectively, sites at which mutations produced WT or indeterminate phenotypes. In (A) and (C), GDP (yellow) can be glimpsed between the two Gα domains (the α-helical domain is colored gray). Ct, COOH-terminal residues 344 to 350 of α_t; not visible in crystals of the heterotrimer (*5*), these are taken from a separate crystal structure (*3*). Nt, NH_2-terminus. (**D** and **E**) Ribbon representations of α_t in a complex (*5*) with subunit β (dark blue; γ not shown). In (D) and (E) α_t is tilted ~90° around the horizontal axis with respect to (A), so that the NH_2-terminal α-helix points toward the viewer. Panel (D) shows locations of sites with an R phenotype, colored as in (A) to (C). Panel (E) highlights structural elements postulated to transmit conformational change from the receptor to the guanine nucleotide–binding pocket. These include α2 and β1 through β3 (cyan), which communicate with βγ, and β6 and α5 (red), proposed as key conformation transmitters between the β6-α5 loop (green, contacting GDP) and parts of the protein that interact directly with membrane-bound receptor, R (α4-β6 loop, mid-α5, and the COOH-terminus).

ing pocket (*11*). We propose (Fig. 3, D and E) that 7TMR-induced changes in the conformations of the β6 strand and the α5 helix are communicated to the β6-α5 loop (green in Fig. 3E), in which side chains of a short sequence of amino acids contact the guanine ring of GDP (*3*, *4*, *18*, *19*).

Although not yet explicitly tested, this idea is in keeping with our present observations and with results of studies that probed functions of β6, α5, and the β6-α5 loop (*20*–*23*). Specifically, several mutations in α5, at locations distant from the nucleotide-binding pocket, increase rates of GDP dissociation and its replacement by GTP (*20*). Amino acid substitutions in the β6-α5 loop increase the GDP dissociation rate in several guanosine triphosphatases (GTPases), promoting spontaneous GTP-for-GDP exchange (*21*–*23*). Such mutations dramatically activate both $p21^{ras}$ and α_s—producing, respectively, neoplastic transformation (*22*) and a human endocrine syndrome, testotoxicosis-pseudohypoparathyroidism (*23*). Thus 7TMR-induced conformational change may be propagated from the membrane through β6 and α5 to the loop that connects them, right in the GDP-binding pocket (Fig. 3, D and E).

REFERENCES AND NOTES

1. H. R. Bourne, D. A. Sanders, F. McCormick, *Nature* **348**, 125 (1990); L. Birnbaumer, *Annu. Rev. Pharmacol. Toxicol.* **30**, 675 (1990); A. H. Cheung, R. R. Huang, C. D. Strader, *Mol. Pharmacol.* **41**, 1061 (1992); M. Freissmuth, P. J. Casey, A. G. Gilman, *FASEB J.* **3**, 2125 (1989); Y. Kaziro, H. Itoh, T. Kozasa, M. Nakafuku, T. Satoh, *Annu. Rev. Biochem.* **60**, 349 (1991); E. J. Neer, *Cell* **80**, 249 (1995).
2. T. M. Vuong, M. Chabre, L. Stryer, *Nature* **311**, 659 (1984); L. Ramdas, R. M. Disher, T. G. Wensel, *Biochemistry* **30**, 11637 (1991).
3. J. P. Noel, H. E. Hamm, P. B. Sigler, *Nature* **366**, 654 (1993).
4. D. G. Lambright, J. P. Noel, H. E. Hamm, P. B. Sigler, *ibid.* **369**, 621 (1994); J. Sondek, D. G. Lambright, J. P. Noel, H. E. Hamm, P. B. Sigler, *ibid.* **372**, 276 (1994); D. E. Coleman *et al.*, *Science* **265**, 1405 (1994); M. A. Wall *et al.*, *Cell* **83**, 1047 (1995).
5. D. G. Lambright *et al.*, *Nature* **379**, 311 (1996).
6. B. K.-K. Fung and C. R. Nash, *J. Biol. Chem.* **258**, 10503 (1983); W. J. Phillips and R. A. Cerione, *ibid.* **267**, 17032 (1992); W. J. Phillips, S. C. Wong, R. A. Cerione, *ibid.*, p. 17040; D. J. Kelleher and G. L. Johnson, *Mol. Pharmacol.* **34**, 452 (1988); O. Kisselev and N. Gautam, *J. Biol. Chem.* **268**, 24519 (1993); A. B. Fawzi *et al.*, *ibid.* **266**, 12194 (1991).
7. Reviewed in B. R. Conklin and H. R. Bourne, *Cell* **73**, 631 (1993).
8. K. A. Sullivan *et al.*, *Nature* **330**, 758 (1987); E. A. Dratz *et al.*, *ibid.* **363**, 276 (1993).
9. H. E. Hamm *et al.*, *Science* **241**, 832 (1988).
10. P. D. Garcia, R. Onrust, S. M. Bell, T. P. Sakmar, H. R. Bourne, *EMBO J.* **14**, 4460 (1995).
11. A supplementary table, available with the *Science* Online version of this report at http://www.sciencemag.org/ lists each of the individual residues mutated, along with their phenotypes, in both rhodopsin interaction assays. The supplement also details the criteria we used to assign WT and R "diagnoses" to each mutant and the procedure for using the AlF_4^- data for normalizing results of the rhodopsin interaction assays. We have reported results of the microsomal assay, but not the in vitro translation assay, for the 10 mutants in the COOH-terminal tail of α_t (*10*).
12. Sites were chosen for mutation if previous work suggested involvement of a particular structural element

in receptor interaction [for instance, the COOH-terminus, α4-β6 loop, and β6 (*7–10*)], if they were known to interact with βγ in the 3D structure of α_t (*5*), or if they were located on the surface of the 3D structure of α_t near either known or postulated rhodopsin- or βγ-interacting residues (*3–5*).
13. S. Osawa and E. R. Weiss, *J. Biol. Chem.* **270**, 31052 (1995).
14. That is, binding values for different mutants in the presence of GTP-γ-S were consistent and small enough not to confound the results. We failed to find a mutant α_t that could bind to rhodopsin but would not be susceptible to rhodopsin-catalyzed replacement of GDP by GTP-γ-S. A mutant rhodopsin with this phenotype has been described (O. P. Ernst, K. P. Hofmann, T. P. Sakmar, *ibid.*, p. 10580).
15. J. Bigay, P. Deterre, C. Pfister, M. Chabre, *FEBS Lett.* **191**, 181 (1985); P. C. Sternweis and A. G. Gilman, *Proc. Natl. Acad. Sci. U.S.A.* **79**, 4888 (1982).
16. The failure of individual mutants to be protected from trypsin by AlF_4^- could indicate improper folding of the protein or an inability of the α2 helix, in which the protected cleavage site is located, to take on the trypsin-resistant (active, GTP-bound) conformation. Of the 66 mutants tested in both assays, only four showed an I phenotype in both. It is likely that overexpression of recombinant α_t in COS cells and its translation in vitro affect folding in different ways.
17. Of the 23 residues identified (*5*) as interacting directly with βγ, we tested 22. By one or the other assay, mutational replacement of 14 of the 22 residues (in 10 mutants) produced an R phenotype, whereas six mutants were WT and two were indeterminable (*11*).
18. O. Lichtarge, H. R. Bourne, F. E. Cohen, *Proc. Natl. Acad. Sci. U.S.A.* **93**, 7507 (1996). In this theoretical study, residues in cluster 2 and cluster 1 correspond, respectively, to the βγ- and putative 7TMR-interacting surfaces identified in the present work.
19. This loop comprises residues 321 to 324 of α_t. Corresponding β6-α5 loops of other GTPases interact similarly with the guanine ring of bound GDP and GTP [H. R. Bourne, D. A. Sanders, F. McCormick, *Nature* **349**, 117 (1991)].
20. B. M. Denker, C. J. Schmidt, E. J. Neer, *J. Biol. Chem.* **267**, 9998 (1992); B. M. Denker, P. M. Boutin, E. J. Neer, *Biochemistry* **34**, 5544 (1995); L. A. Quilliam *et al.*, *Proc. Natl. Acad. Sci. U.S.A.* **92**, 1272 (1995).
21. T. C. Thomas, C. J. Schmidt, E. J. Neer, *Proc. Natl. Acad. Sci. U.S.A.* **90**, 10295 (1993).
22. L. A. Feig and G. M. Cooper, *Mol. Cell. Biol.* **8**, 2472 (1988).
23. T. Iiri, P. Herzmark, J. M. Nakamoto, C. Van Dop, H. R. Bourne, *Nature* **371**, 164 (1994).
24. An indirect effect of alanine substitution is especially likely for the few residues we tested whose side chains are directed toward the protein's hydrophobic core; these include two phenylalanine residues, colored cyan (F185) or red (F332) in Fig. 3, A through C. We considered four additional R residues (green in Fig. 3, A through C), scattered through the α_t molecule, as quite unlikely to interact directly with βγ or rhodopsin. Residues Gly^2 and Ser^6 are required for myristoylation of α_t, which in turn is necessary for efficient activation [P. J. Casey, *Curr. Opin. Cell Biol.* **6**, 219 (1994)]. Residues Thr^{323} and Asp^{324} are located very close to the guanine nucleotide–binding pocket (*3–5*), where they might be expected to alter regulation of GTP-GDP exchange.
25. We thank members of our laboratories for helpful discussions and reading of the manuscript, H. Czerwonka for preparing the manuscript, H. Hamm (University of Illinois at Chicago) for a sample of rod outer segment membranes, and B. K.-K. Fung (Jules Stein Eye Research Institute, Los Angeles, CA) for the TF15 monoclonal antibody used for α_t immunoblots. R.O. is a Helen Hay Whitney fellow, P.C. was supported by a grant from the Genentech Foundation, P.D.G. was supported in part by funds from Daiichi, and O.L. was supported by funds from the American Heart Association. Supported by NIH grants GM-27800 and CA-54427 (to H.R.B.).

27 August 1996; accepted 12 November 1996

Consumer Versus Resource Control in Freshwater Pelagic Food Webs

Michael T. Brett* and Charles R. Goldman

Models predict that food-web structure is regulated by both consumers and resources, and the strength of this control is dependent on trophic position and food-web length. To test these hypotheses, a meta-analysis was conducted of 11 fish (consumer)-by-nutrient (resource) factorial plankton community experiments. As predicted, zooplankton biomass was under strong consumer control but was weakly stimulated by nutrient additions; phytoplankton biomass was under strong resource control with moderate control by fish. However, the phytoplankton and zooplankton responses to nutrient additions did not follow theoretical predictions based on the number of trophic levels in the food web.

The nature of the factors regulating food-web structure has been a very active area of ecological research (*1, 2*) since the classic paper by Hairston, Smith, and Slobodkin (*3*) was published in 1960. In aquatic systems, food-web interactions strongly influence fisheries production, biogeochemical cycling, and ecosystem responses to anthropogenic eutrophication. A recent quantitative summary of the freshwater trophic cascade (*4*) literature showed that planktivorous fish treatments result in decreased herbivore (zooplankton) and increased primary producer (phytoplankton) biomass (*5*). In addition, phytoplankton response to the cascade is weakly dampened and highly variable, with weak responses in two-thirds of the experiments and very strong responses in the other experiments (*5*). Still, many questions regarding the dynamic nature of food-web interactions remain unresolved (*1, 2*). In particular, what is the relative strength of consumer and resource control in pelagic food webs (*6*), and how do food webs respond to changes in system productivity under different food-web configurations (*7*)?

The debate over top-down (consumer) versus bottom-up (resource) control represents a synthesis of the known impact of nutrient regulation of primary producers (*8*) and higher trophic levels (*9*), and the more recent emphasis on consumer control of trophic levels through the cascade (*4*). In essence, the debate centers on whether herbivore and plant communities are regulated through predator control of herbivore abundance or through nutrient control of primary production. McQueen and colleagues (*6*) predicted bottom-up control is stronger at the base of the food web, and top-down control is stronger at higher trophic levels. For example, the zooplankton should be more strongly controlled by zooplanktivorous fish than by nutrients, whereas phytoplankton biomass should be primarily controlled by nutrient availability and to a lesser extent by higher trophic levels.

Oksanen *et al.* (*7*) developed a series of models to explore the theoretical relationship among ecosystem productivity, patterns of biomass accrual, and the number of trophic levels in that ecosystem. This predicted "a stepped pattern of biomass accrual" (*2*) across productivity gradients (*10*). In food webs with an odd number of trophic levels, increases in primary production should lead to increased biomass for odd-numbered trophic levels and no change in biomass for even-numbered trophic levels. Conversely, in food webs with an even number of trophic levels, increases in primary production should lead to increased biomass for even-numbered trophic levels and no change in biomass for odd-numbered trophic levels.

We assembled eight studies (*11*) that reported the results of 11 independent mesocosm experiments employing factorial nutrient addition and zooplanktivorous fish treatments. Simple criteria were used to decide which studies to include in our analysis (*12*). Six of the studies used simple fish-by-nutrient designs, and two used slight modifications of this design (*13*). In five studies, zooplankton community biomass values were obtained directly, and in three studies, zooplankton biomass was estimated using abundance and individual biomass data (*14*). All phytoplankton community biomass values were taken directly from the respective studies.

Mesocosms are classic experimental de-

Division of Environmental Studies, University of California, Davis, CA 95616, USA.

*To whom correspondence should be addressed. E-mail: mtbrett@ucdavis.edu